

Quantum Transport of Massless Dirac Fermions in Graphene

Kentaro Nomura and A. H. MacDonald

Department of Physics, University of Texas at Austin, Austin TX 78712-1081, USA

(Dated: February 8, 2020)

Motivated by recent graphene transport experiments, we have undertaken a numerical study of the conductivity of disordered two-dimensional massless Dirac fermions. We find that in the short-range scattering case the minimum conductivity $\sigma^{\min} \approx (1/\pi)e^2/h$, while in the case of Coulomb scattering due to ionized impurities $\sigma^{\min} \approx e^2/h$. We address an essential difference between these two cases, that is, the Dirac point of massless Dirac fermion model remains in the clean limit even in the presence of the short-range scattering, while Coulomb scatterers turn it into the strong disorder limit.

PACS numbers: 72.10.-d, 73.21.-b, 73.50.Fq

Introduction— Graphene can be described at low-energies by a four component massless Dirac-fermion (MDF) model[1] that has long attracted theoretical attention because of appealing properties including chiral anomalies[2, 3, 4, 5], randomness induced quantum criticality[6, 7, 8, 9], unusual electron-electron interaction effects[10, 11], relevance to high T_c superconductors[10, 12], and various unusual transport properties[5, 6, 7, 8, 9, 10, 11, 12, 13, 14, 15, 16, 17, 18, 19, 20, 21]. The recent experimental realization of single-layer graphene sheets[22] has made it possible to confirm a number of theoretical predictions, including unusual half-integer quantum Hall effects[23, 24], and has also revealed some surprises. The main findings can be summarized as follows: i) graphene’s conductivity σ never falls below a minimum value (σ^{\min}) corresponding (approximately) to a conductance quantum (e^2/h) per channel, in spite of theoretical[6, 7, 12, 13, 14, 15, 17] predictions that $\sigma^{\min} \approx (1/\pi)e^2/h$ for a MDF channel and that localization occurs[18, 19] when intervalley scattering is significant; ii) in gate-doped graphene σ increases linearly with carrier density away from the charge neutrality (Dirac) point, implying a constant mobility $\sigma = ne\mu$ [23, 24] and not the constant conductivity predicted for the Boltzmann transport regime[15]. Although these surprises have inspired a number of theoretical studies[17, 18, 19], the source of the discrepancies between experiment and theoretical predictions has not yet been conclusively identified. Significantly it has been argued theoretically that the nature of zero energy states does not change even in the presence of disorder, and that the conductivity at the Dirac point retains the MDF disorder-free value $(1/\pi)e^2/h$.

We have recently pointed out that the linear dependence of conductivity on carrier density in graphene can be explained in the framework of Boltzmann transport theory by assuming Coulomb scatterers[25] rather than the short-range scatterers assumed in most theoretical work mainly as a practical simplification. Here we note that the scattering rate for Coulomb scatterers in a MDF model diverges in the zero energy (Dirac point)

limit, whereas it vanishes for short-range scatterers. This property suggests that the Dirac point is in the strong disorder limit for Coulomb scatterers and not in the weak disorder limit as in a MDF short-range scattering model. Since Boltzmann theory is not applicable in the vicinity of the Dirac point, a fully quantum mechanical approach is required to address the minimal conductivity. In this Letter we report on a finite-size Kubo formula analysis used to study the quantum transport of MDFs. We find that for Coulomb scatterers $\sigma^{\min} \approx e^2/h$ (in agreement with graphene experiment if inter-valley scattering is unimportant) while short-range scatterers lead to $\sigma^{\min} = (1/\pi)e^2/h$ as predicted by theory[6, 7, 12, 13, 14, 15, 17]. Our two-component MDF model is relevant to zero-field graphene transport when inter-valley scattering is unimportant. We argue that this condition is likely to be fulfilled in the vicinity of the Dirac point, where the inter-valley scattering length obtained within the Born approximation diverges. In the highly doped regime, on the other hand, inter-valley scattering is more likely to be important at accessible temperatures, accounting for a recent magnetoresistance study[26].

Massless Dirac Fermion Model— Graphene’s honeycomb lattice has two atoms per unit cell on sites labeled A and B . The low-energy band structure consists of Dirac cones located at the two inequivalent Brillouin zone corners K and K' :

$$H_K = \hbar v \boldsymbol{\sigma} \cdot \mathbf{k} = v \hbar \begin{pmatrix} 0 & k_x - ik_y \\ k_x + ik_y & 0 \end{pmatrix}, \quad (1)$$

and $H_{K'} = \hbar v \boldsymbol{\sigma}^t \cdot \mathbf{k}$, where v is the graphene Fermi velocity and the Pauli matrices $\boldsymbol{\sigma}$ act on the sublattice degrees of freedom. For each wavevector \mathbf{k} , Eq.(1) has two eigenstates $|\mathbf{k}, \pm\rangle = (|\mathbf{k}, A\rangle \pm e^{i\phi}|\mathbf{k}, B\rangle)/\sqrt{2}$, where $\phi \equiv \tan^{-1}(k_y/k_x)$, and eigenenergies $E_{\mathbf{k}, \pm} = \pm v\hbar|\mathbf{k}|$. In this Letter we neglect inter-valley scattering and can therefore treat the inequivalent K points independently. *Boltzmann theory for doped graphene*—We start by briefly reviewing Boltzmann transport theory applied to graphene since this consideration motivates the in-

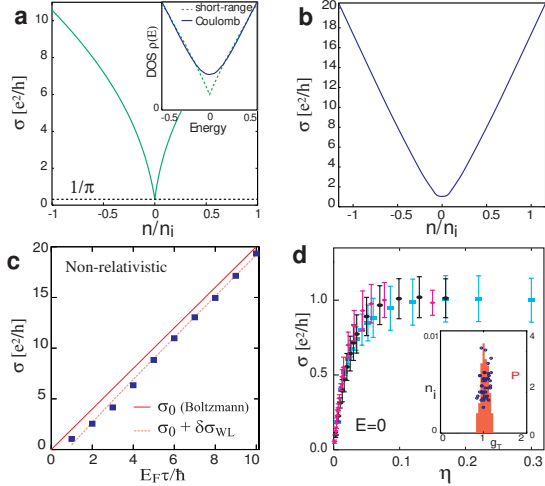


FIG. 1: Dirac fermion conductivities for (a) short-range scatterers and (b) screened Coulomb scatterers. The inset of (a) compares the densities of states for short-range and Coulomb cases. (c) compares the Drude conductivity without (solid line) and with (dashed line) weak-localization corrections with the finite-size Kubo formula results (boxes) in a conventional non-relativistic two-dimensional fermions system calculated with the same approach we apply here to the MDF model. (d) shows Kubo formula conductivities at the Dirac point for three different system sizes as a function of η for Coulomb scatterers. The inset of (d) shows the Thouless number at the Dirac point as a function of the density of Coulomb scatterers.

introduction of long-range disorder models. The Boltzmann conductivity $\sigma_0 = (e^2/h) (2E_F\tau/\hbar) = (e^2/h) 2k_F l$ is proportional to the transport relaxation time τ_0 . For short-range scatterers the Born approximation gives $\hbar/\tau_0 = 2\pi\overline{V^2}\rho_F = (n_i u^2/\hbar v^2) |E_F|$ [15], where $V(\mathbf{r}) = u \sum_I^{N_i} \delta(\mathbf{r} - \mathbf{R}_I)$ is the disorder potential, $\overline{V^2} = N_i u^2$, $N_i = n_i L^2$ is the number of scatterers, L is the size of the system, and ρ_F the density of states at the Fermi level. When the range of the impurity potential is much longer than the lattice spacing of graphene, inter-valley scattering is weak[15, 16, 18]. Note that σ_0^s is independent of the carrier density n . Experiment, on the other hand, finds that the mobility $\mu = \sigma/ne$ in graphene is nearly constant except at very low-densities. One plausible explanation for this behavior is that Dirac fermion scattering is dominated by Coulomb scattering from ionized impurities near the graphene plane, $V(\mathbf{r}) = \sum_I^{N_i} e^2/|\mathbf{r} - \mathbf{R}_I|$. Using Fermi's golden rule, and approximating the screened Coulomb interaction by[25] $U_{sc}(\mathbf{q}) = (2\pi e^2)/(q + 4gk_F) \simeq (\hbar v \pi)/(2k_F)$ the Boltzmann conductivity for Coulomb interactions is $\sigma_0^c \simeq (4e^2/h) (n/n_i) 32/\pi$, proportional to density in agreement with experiment. Here $g = e^2/\hbar v$ is the effective fine structure constant used to characterize the ratio of Coulomb interaction and band energy scales in graphene.

($g \simeq 3$ in vacuum and $\simeq 1$ when the graphene sheet is placed on a dielectric substrate.) Note that the Boltzmann conductivity for Coulomb scatterers vanishes as $n \rightarrow 0$, contradicting experiment[23].

Linear response theory for the Dirac fermion – Our numerical results for zero-field transport are summarized in Fig.1. These results were obtained by evaluating the finite-size Kubo formula:

$$\sigma = -\frac{i\hbar e^2}{L^2} \sum_{n,n'} \frac{f(E_n) - f(E_{n'})}{E_n - E_{n'}} \frac{\langle n|v_x|n' \rangle \langle n'|v_x|n \rangle}{E_n - E_{n'} + i\eta}, \quad (2)$$

where $\mathbf{v} = v\boldsymbol{\sigma}$ is the Dirac fermion velocity operator, $f(E)$ is the Fermi-Dirac function at $T = 0$, and $|n\rangle$ denotes an eigenstate of the Dirac equation,

$$\left[-i\hbar\mathbf{v}\boldsymbol{\sigma} \cdot \nabla + V(\mathbf{r}) \right] \psi = E\psi \quad (3)$$

which we solve using a large momentum-space cutoff Λ . The matrix elements of the disorder potential term are given in momentum-psendospin space by

$$\langle \mathbf{k}\sigma | V | \mathbf{k}'\sigma' \rangle = \frac{1}{L^2} \sum_{I=1}^{N_i} U(\mathbf{k} - \mathbf{k}') \delta_{\sigma\sigma'} e^{i(\mathbf{k}-\mathbf{k}') \cdot \mathbf{R}_I}, \quad (4)$$

where $U(\mathbf{q})$ is constant and for delta-impurities and given by $U_{sc}(\mathbf{q})$ for the screened Coulomb scattering case, and the scattering centers \mathbf{R}_I are the potential signs are random. The results shown in Fig.1 are typically averaged over 10^4 disorder realizations. We estimate the bulk conductivity by evaluating Eq.(2) at a large number of η -values. The Kubo conductivity σ vanishes for both small and large η but there is a region where σ becomes finite and its dependence on η is relatively weak. We use the maximum of σ as a function of η to estimate the conductivity at a given system size L . For metals, including doped graphene, physical arguments suggest that $\eta \sim \hbar/T$ where T is the escape time from the system studied numerically. It follows[27] that $\eta \sim \langle \Delta E \rangle \sim g_T \delta E$, where the Thouless energy $\langle \Delta E \rangle$ is the geometric mean of the eigenvalue difference between periodic and antiperiodic boundary conditions, $\delta E = 1/L^2 \rho_F$ is the level spacing at the Fermi level, and $g_T \equiv \langle \Delta E \rangle / \delta E$ is the Thouless number.

The reliability of the finite-size Kubo formula method described above is solidly established for diffusive metallic systems[27]. For example typical results obtained when the methods employed here for the MDF model are applied to a conventional (non-relativistic) two-dimensional electron system are shown in Fig.1(c). The numerical agree closely with the theoretical expectation of a Drude conductivity $\sigma_0 = (e^2/h)k_F l = (e^2/h)2E_F\tau$ (solid line) with a finite-size weak-localization correction[28]. Subtleties do arise, however, when this method is applied to insulators. The Dirac point is intermediate and we acknowledge this as an

issue in the interpretation of our calculations. (The property that the Dirac point density of states is finite in the presence of disorder, as illustrated in the inset of Fig.1(a), should help validate the Kubo approach.) For this reason we have also evaluated the Thouless conductivity as a consistency check. A large number of numerical studies have demonstrated that the Thouless conductivity estimate, although perhaps not as accurate in the diffusive metal limit ($\sigma \gg e^2/h$), is more universally applicable. It may be used for both delocalized and strongly localized states[29], and should therefore be reliable at the Dirac point. The inset of Fig.1 (d) and Fig.1 (d) establish the consistency of these two conductivity estimates and support the reliability of our numerical results for σ^{\min} . The dependence of the disorder averaged σ on η is shown in Fig.1(d) for three different system sizes at the Dirac point. We find that the η -dependence of the Kubo formula estimate at the Dirac point is similar to that in a metal[27], indicating delocalized states. σ becomes maximal when η corresponds to $\sim \delta E$ at each system size in agreement with these considerations.

Figure 1 compares Kubo conductivity estimates for (a) the short-range scatterer and (b) the screened Coulomb scatterer cases. For the short-range disorder potential case, the density dependence of the conductivity is non-linear, approaching the constant Boltzmann conductivity for $|E_F| \gg \hbar/\tau$. The estimated value of $\sigma^{\min} \simeq (1/\pi)e^2/h$ as predicted in earlier theoretical studies[6, 7, 12, 13, 14, 15, 17]. For the screened Coulomb scatterer case, on the other hand, the conductivity σ increases linearly with increasing density $|n|$ as Boltzmann theory predicts. At the Dirac point, however, the conductivity remains finite with the minimum value $\simeq e^2/h$. If we neglect inter-valley disorder scattering and account for the spin degeneracy and valley degeneracy for graphene, this MDF result can be compared with graphene experimental results. Both the linear dependence of the conductivity on density and the shift of σ^{\min} suggest that long-range scattering similar to that produced by ionized impurities is present in experimental samples. We note that ionized impurities in the substrate or at samples edges that are separated from the conduction channel by a distance that is large compared to the graphene lattice constant but small compared to the Fermi wave length in the regime studied experimentally ($|n| \lesssim 7 \times 10^{12}[\text{cm}^{-2}]$ [23, 24]) will act like Coulomb scatterers in the MDF model but will not produce strong inter-valley scattering.

To illustrate the dependence on carrier density, we have smoothed the curves in Fig.1(a) and (b) by averaging over Fermi energy interval containing typically 1-30 levels, and over boundary conditions, in addition to over approximately 10^4 disorder realizations. To illustrate the statistical character of conductivity near the Dirac point, we plot the disorder averaged Kubo conductivity as a function of η for three different system sizes in Fig.1(c)

(with 400, 628, and 904, momentum-space basis states respectively). The error bars indicate the scale of fluctuations associated with changing the number of states in the finite systems by ~ 1 . Note that the mean value is close to e^2/h . The inset of Fig.1(d) summarizes our results for the Thouless number at the Dirac point. The overall distribution function demonstrates that σ_T^{\min} is narrowly peaked near e^2/h . The dependence on the density of Coulomb scatterers is indicated by the scatter plot which shows conductivity values calculated at particular n_i values. These results suggest that the MDF σ^{\min} for Coulomb scatterers equals e^2/h to within approximately 15%. We do not find evidence for a decrease of the minimal conductivity with increasing systems size in either Kubo and Thouless approaches over the range of systems sizes that we are able to study, indicating that the states at the Dirac point are delocalized.

The difference between Coulomb and short-range disorder σ^{\min} values can be explained qualitatively by the following argument. In the short-range case, the golden-rule relaxation time for delta-function scatterers diverges ($\tau_0 \propto 1/|E_F| \rightarrow \infty$) at the Dirac point, which suggests that the $E = 0$ state is always in the clean limit. Indeed, it is significant to note that the universal conductivity at the Dirac point in this model is equal to the conductivity of a disorder-free system[6, 7]. (The conductivity is finite in the absence of scattering because the density of states vanishes at the Dirac point.) In contrast, Boltzmann transport theory suggests that the Dirac point of the Coulomb scatterer model is in the strong disordered limit because $\tau_c \propto |E_F| \rightarrow 0$. As long as these states remain delocalized, however, the conductivity cannot vanish; the non-zero conductivity at the Dirac point is purely due to the quantum mechanical nature of delocalized states. Although this argument cannot provide a numerical estimate for the Coulomb case, it makes it clear that there is an essential difference between these two cases. A related difference is also seen in the inset in Fig.1(a) which compares densities of states near the Dirac point ($E = 0$) for short-range scatterers (green dashed line) and Coulomb scatterers (blue solid line). The prominent dip at $E = 0$ in the short-range case is replaced by a smooth minimum at a larger value in the Coulomb case. One interpretation of the increase in Dirac point density of states is that the carrier density fluctuates spatially in the smooth Coulomb potential. Non-zero local carrier densities could explain both the increase in density of states and the increase in conductivity. We examined this idea by varying the carrier density n and the ionized impurity density n_i independently, finding that the conductivity for Coulomb scattering model appears to be a function of n/n_i only. Letting $n \rightarrow 0$ at finite n_i and letting $n_i \rightarrow \infty$ at finite n are equivalently because $\sigma \rightarrow \sigma^{\min} \simeq e^2/h$. This finding is consistent with the idea that at the Dirac point MDF Coulomb scatterers are always in the strongly disordered limit.

Discussion – We find that a massless Dirac fermion model with Coulomb scatterers is able to account for two key findings of experiments on graphene sheets, namely that the conductivity is proportional to carrier density away from the Dirac point and that the minimal conductivity per channel is finite and close to e^2/h , several times larger than the universal value obtained theoretically for a MDF model with short-range scatterers. The impurity density n_i in the Coulomb model should be associated with the density of ionized impurities that are located in the substrate within a Fermi wavelength of the graphene plane. In this interpretation, the mobilities measured in current samples[23, 24] corresponds to $n_i \simeq 5 \times 10^{11} \text{ [cm}^2\text{]}$. The property that the conductivity is proportional to carrier density in the Boltzmann regime suggests dominant smooth intra-valley scattering that could be Coulombic in character. Although intervalley scattering does not appear to be important in the Boltzmann regime, it is much more likely to be relevant for weak localization corrections at low temperatures. Relevance for weak localization requires only that the intervalley scattering length be shorter than the phase coherence length, whereas relevance in the Boltzmann regime requires that it be comparable to the overall mean free path. Since the inter-valley scattering length is $l_0 \propto 1/|E_F|$ inter-valley scattering is more important for high doping than in the vicinity of the Dirac point. When intervalley scattering is weak, the MDF model applies and momentum space Berry phases change constructive interference of back scattering particles into destructive interference[16, 30]. When Dirac fermions are simulated on a lattice system with random sites, intra- and inter-valley scattering rates are same order of magnitude[15, 16, 18], accumulated Berry phases are randomized, and all states are localized.[13, 21] Qualitative studies of electron-phonon interaction[31] and electron-electron interaction[11] in graphene can give important information on the coherence length. In a weak magnetic field, the magnetic length limits the coherence length. One recent magnetoresistance study has shown that highly doped graphene exhibits a negative magneto resistance indicating weak-localization, while states remain delocalized in the vicinity of the Dirac point. [26] In the presence of mesoscopic ripples in samples, the quantum corrections are strongly suppressed. We conclude from the occurrence of a minimum metallic conductivity in current graphene samples that inter-valley scattering is not significant at the Dirac point, and from the present work that the anomalous value of this minimum conductivity is due to smooth Coulomb-like scatterers.

Acknowledgment – The authors acknowledge helpful interactions with A. Geim, T. Hughes, Z. Jiang, P. Kim, V. Falko and A. Castro-Neto. This work has been supported by the Welch Foundation and by the Department of Energy under grant DE-FG03-02ER45958.

Note added – After submitting the present paper, we became aware of related work in which the impor-

tance of the long-range nature of disorder scatterers is discussed.[32, 33]

- [1] J. C. Slonczewski and P. R. Weiss, Phys. Rev. **109**, 272 (1958).
- [2] S. Deser, R. Jakiew, and S. Templeton, Phys. Rev. Lett. **48**, (1982) 975.
- [3] G.W. Semenoff, Phys. Rev. Lett. **53**, 2449 (1984)
- [4] E. Fradkin, E. Dagotto D. Boyanovsky, Phys. Rev. Lett. **57**, (1986) 2967.
- [5] F.D.M. Haldane, Phys. Rev. Lett. **61**, 2015 (1988);
- [6] E. Fradkin, Phys. Rev. B **33**, 3263 (1986)
- [7] A. W. W. Ludwig, M. P. A. Fisher, R. Shankar, and G. Grinstein, Phys. Rev. B 50, 7526 (1994).
- [8] Y. Hatsugai and P. A. Lee, Phys. Rev. B **48**, 4204 (1993).
- [9] C. de C. Chamon *et al.*, Phys. Rev. Lett. **77**, 4194 (1996).
- [10] D.H. Kim *et al.*, Phys. Rev. Lett. **79**, 2109 (1997).
- [11] D. V. Khveshchenko, Phys. Rev. Lett. **87**, 206401 (2001); J. Gonzalez *et al.*, Phys. Rev. B **63**, 134421 (2001); T. Stauber *et al.*, Phys. Rev. B **71**, 041406 (2005); Khveshchenko, cond-mat/0604180.
- [12] P.A. Lee, Phys. Rev. Lett. **71**, 1887 (1993).
- [13] Y. Morita and Y. Hatsugai, Phys. Rev. Lett. **79**, 3728 (1997); Phys. Rev. B **58**, 6680 (1998).
- [14] K. Ziegler, Phys. Rev. Lett. **80**, 3113 (1998)
- [15] N.H. Shon and T. Ando, J. Phys. Soc. Jpn. **67** (1998) 2421.
- [16] H. Suzuura and T. Ando, Phys. Rev. Lett. **89**, 266603 (2002).
- [17] N. M. R. Peres, F. Guinea, A. H. Castro Neto, Phys. Rev. B **73**, 125411 (2006).
- [18] E. McCann, K. Kechedzhi, Vladimir I. Fal'ko, H. Suzuura, T. Ando, B.L. Altshuler, cond-mat/0604015; D.V.Khveshchenko, Phys. Rev. Lett. **97**, 036802 (2006); A. F. Morpurgo, F. Guinea, cond-mat/0603789.
- [19] K. Ziegler, cond-mat/0604537; I.L. Aleiner, K.B. Efetov, cond-mat/0607200; A. Altland, cond-mat/0607247.
- [20] A.M.J. Schakel, Phys. Rev. D **43**, 1428 (1991); Y. Zheng and T. Ando, Phys. Rev. B **65**, 245420 (2002); V.P. Gusynin and S.G. Sharapov, Phys. Rev. Lett. **95**, 146801 (2005).
- [21] D.N. Sheng *et al.*, Phys. Rev. B **73**, 233406 (2006).
- [22] K.S. Novoselov *et al.*, Science **306**, 666 (2004).
- [23] K.S. Novoselov *et al.*, Nature **438**, 197 (2005)
- [24] Y.B. Zhang *et al.*, Nature **438**, 201 (2005).
- [25] K. Nomura, A.H. MacDonald, Phys. Rev. Lett. **92** 256602 (2006).
- [26] S.V. Morozov, K.S. Novoselov, M.I. Katsnelson, F. Schedin, D. Jiang, A.K. Geim, Phys. Rev. Lett. **97**, 016801 (2006).
- [27] D. J. Thouless and S. Kirkpatrick, J. Phys. C, 14, 235 (1981), Y. Imry, *Introduction to Mesoscopic Physics*, Oxford University.
- [28] P.A. Lee and T.V. Ramakrishnan, Rev. Mod. Phys. **57**, 287 (1985).
- [29] T. Ando, J. Phys. Soc. Jpn. **52**, 1740 (1983); **53** 3101 (1984); **53** 3126 (1983).
- [30] T. Ando, T. Nakanishi, R. Saito, J. Phys. Soc. Jpn. **67**, 2857 (1998).
- [31] A. H. Castro Neto, F. Guinea, cond-mat/0608543.

[32] H. Kumazaki and D. S. Hirashima: *J. Phys. Soc. Jpn.* **75**, 53707 (2006).

[33] T. Ando, *J. Phys. Soc. Jpn.*, **75**, 74716 (2006).